Uluslararası Mühendislik Araştırma ve Geliştirme Dergisi
International Journal of Engineering Research and Development

UMAGD, (2023) 15(2), 610-614

10.29137/umagd.1286392

Cilt/Volume:15 Sayı/Issue:2 Haziran/June 2023

Araştırma Makalesi / Research Article

3B Baskılanmış Bir Kanalda Sıvı Basıncının Damlacık Boyutu İle İlişkisi

Correlation Of Fluid Pressure And Microdroplet Size In A 3D-Printed Microfluidic Chip

Mustafa Tahsin Güler[1]

[1]*Kırıkkale Üniversitesi Fen Edebiyat Fakultesi Fizik Bölümü, 71450 Yahşihan/Kırıkkale, Türkiye*

Başvuru/Received: *21/04/2023* ***Kabul / Accepted***: *13/05/2023* ***Çevrimiçi Basım / Published Online:*** *30/06/2023*
Son Versiyon/Final Version: *30/06/2023*

Öz
Bu makale 3B baskılanmış bir mikro kanalada damlacık oluşumunun sıvı basıncı ile olan ilişkisini inceler. SLA (stereyolitografi) 3B yazıcı ile reçineden şefff mikroakışkan çip imal edilmiştir. Yağ içinde su mikro damlacıkarı sıvı odaklama tasarımında oluşturulmuştur. Yağ ve su girişleri sabit basınç kayanağı ile sürülmüştür. Mikroakışkan çipin mikrodamlacık oluşturma başarımı mikroskop vasıtasıyla gözlenmiştir. Mikrodamlacıkların boyutları sıvı basıncına göre belirlenmiştir.

Anahtar Kelimeler
"Mikroakışkanlar, 3B baskı, Mikrodamlacık"

Abstract
This paper reports the droplet formation performance of a 3D-printed microfluidic chip according to fluid pressure. SLA (stereolithography) 3D printer was employed for manufacturing the transparent microfluidic chip from resin. Water in oil microdroplets was produced on a flow-focusing design. Oil and water inlets were driven by a constant pressure source. The droplet production performance of the microfluidic chip was monitored through a microscope. The size of water droplets was determined according to pressure values.

Key Words
"Microfluidic, microdroplet, 3D-printing"

1. Introduction

Microfluidics open an era for fast and more inexpensive analysis systems which are known as micro total analyzing systems (µTAS). Disease diagnosis (Wu, et al. 2017), determination of antibiotic resistance (Ghorbanpoor, et al. 2022), molecular tests such as PCR (Li, et al. 2023) and LAMP (Oliveira, et al. 2020), as well as organ on a chip (Wu, et al. 2020), are among the applications of microfluidics. Microchannels, which are at the core of µTAS have challenging fabrication methods that require a cleanroom process. Yet, the invention of soft lithography enabled more researchers to access the field of µTAS technology. However, the need for clean rooms remained a drawback of soft lithography. Therefore, recently developed methods started to enable the clean room-free fabrication of microchannels.

Laser machining is one of the most widely adopted alternatives for microchannel manufacturing. It is possible to machine microchannel down to 1 µm resolution (Kim, et al. 2005) through a femtosecond laser. In comparison to soft lithography, which offers 0.5 µm resolution, femtosecond laser machining is a good but expensive alternative that also enables 3D engraving. CO_2 laser machining offers a relatively cost-effective microchannel manufacturing from thermoplastic (Bilican and Guler 2020) or PDMS (Guler 2022). It is also possible to engrave microchannel mold from PMMA (Guler, et al. 2021) or PDMS (Isiksacan, et al. 2016) by CO_2 laser machining.

***Sorumlu Yazar:** gulermt@kku.edu.tr*

The invention of 3D printing led the researcher to employ 3D printers to make microchannels. Fabrication of transparent microchannel was shown employing a Fused deposition modeling (FDM) 3D printer (Nelson, et al. 2019). In another work, multi-jet modeling (MJM) 3D printing was shown to make a T-junction microchannel (Donvito, et al. 2015). Also, SLA 3D printing method was used to fabricate transparent microchannels for biological application (Kecili and Tekin 2020; Lepowsky, et al. 2018). Alternative materials, such as perfluoropolyether, were also shown to be useful in SLA 3D printing of transparent microchannels (Kotz, et al. 2018).

Droplet production in T-junction and flow-focusing geometry has been shown for FDM 3D-printed microchannels (Morgan, et al. 2016; Tsuda, et al. 2015). Bhargava et. al. showed the fabrication of microfluidic elements via SLA 3D printer to produce and sense microdroplets (Bhargava, et al. 2014). Jans et. al. showed the fabrication of parallelized 3D microchannel for multiple productions of microdroplets via SLA 3D printing. This paper presents the droplet production performance of an SLA 3D-printed microchannel. Constant pressure sources generated a flow of oil and water phase inside the channel. According to the pressure value, droplet size was investigated. The upper and lower pressure value of water for a fixed oil pressure value was determined.

2. Materials and Methods

2.1 Fabrication of microchannels

Microchannels were designed at a computer-aided design program (Fusion 360). The microchannels were printed using an SLA 3D printer (Formlabs, Form 3) from clear resin (Formlabs, Clear V4). The design file was transferred to the SLA slicer (Formlabs, Preform 3.28.1) in STL format. The designed microchannel and its orientation in the Preform are shown in Figure 1. Microchannels were printed directly over the build platform without any raft; 25 µm layer thickness was adapted in legacy print settings. Fluid inlet outlet holes were designed as 2.3 mm in diameter. Microchannels were designed as 400 x 400 µm square profiles.

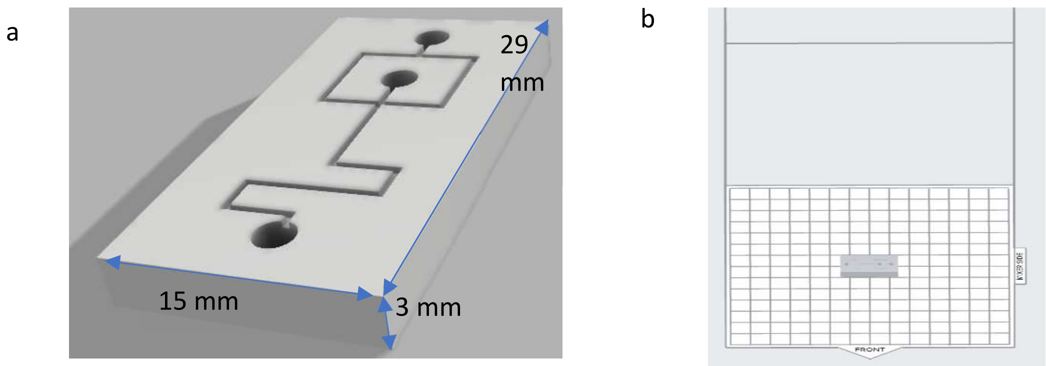

Figure 1 (a) View of the microchannel in CAD file **(b)** microchannel directly placed over the build platform in Preform software.

The 3D-printed parts were taken from the build platform via scalpel and dipped into isopropyl alcohol (IPA) for 30 minutes. Generally, the vent of the holes that are on the side, stuck to the build platform, were closed with a very thin layer of cured resin. The vent was opened using a pick and the 3D printed parts were washed under tap water and DI water respectively and dried with pressurized air. The 3D printed parts were dipped into the IPA again for 5 minutes and then washed with DI water and dried with pressurized air. The 3D printed parts were post-cured with a 405 nm wavelength UV lamp for 2 hours. After curing, 3D-printed microchannels were sealed with tape (3M crystal) from one side.

2.2 Flow in Microchannels

Fluid connections were done using silicon (Cole Palmer) or Tygon tubing (Cole Palmer) that have 0.094 inches outer diameter as shown in Fig. 2. For the connection of silicon tubing, the tip of the tubing should be cut inclined in order to fit into the hole. As the Tygon tubing is not as smooth as silicon, it doesn't need such a cutting process. DI water was mixed with red food dye to provide better monitoring. SF 100 silicon oil (Ultrakim, Ultrasil) was used as the other phase of the flow. Both DI water and silicon oil were put inside a 20 ml vial and connected to a computer-controlled pressure pump (Elveflow, OB1). Flow through the microchannel was monitored through an optical microscope.

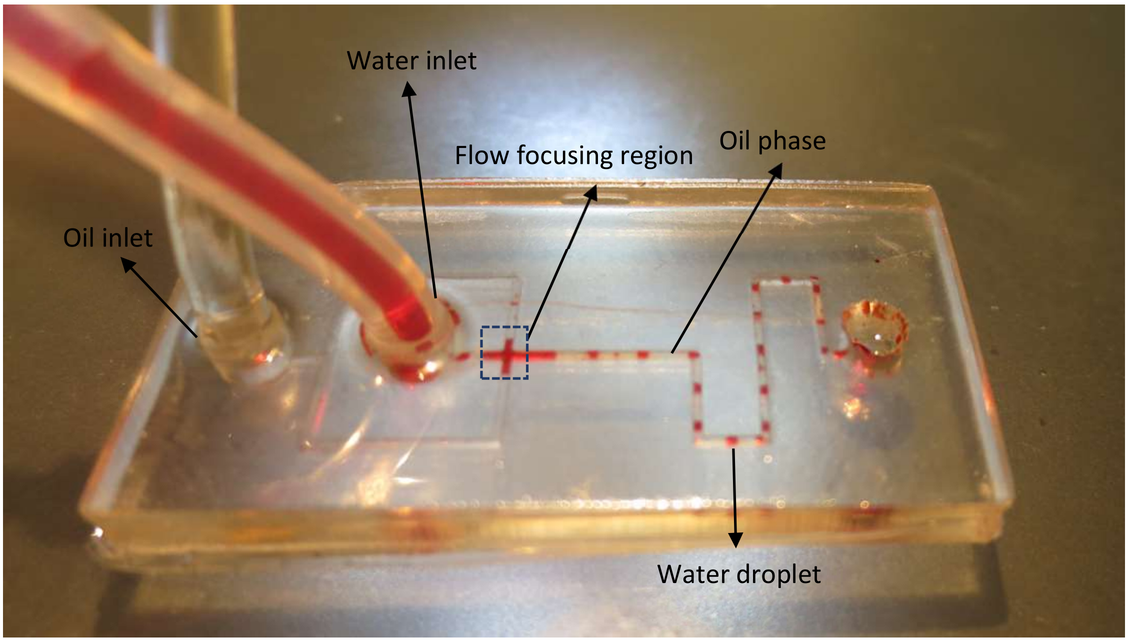

Figure 2 3D printed microfluidic chip with fluidic connection

3. Results and Discussions

3.1 Effect of pressure on droplet formation

Microdroplets were formed in flow-focusing geometry for several oil and water pressures. 100 mbar oil pressure was determined as the oil pressure for this work as it is neither too low nor too high. The produced water in oil microdroplets is shown in Fig. 3a. The droplets were formed at four different pressures of water from low to high. The low water pressure was 45 mbar and the high-water pressure was 60 mbar. On a fixed oil pressure of 100 mbar, when the water pressure was increased, the length of water droplets was increased; when the water pressure was decreased then the length of droplets was decreased as shown in Fig 3b. Above 63 mbar and below 45 mbar no stable droplet formation was achieved. Below 45 mbar water flow stopped and above 63 mbar two-phase flow evolved to continuous flow. This phenomenon can be explained by the hydrophilicity of the resin microchannel, unlike the PDMS microchannel. At the PDMS microchannel, the pressure range is wider which enables more different droplet sizes.

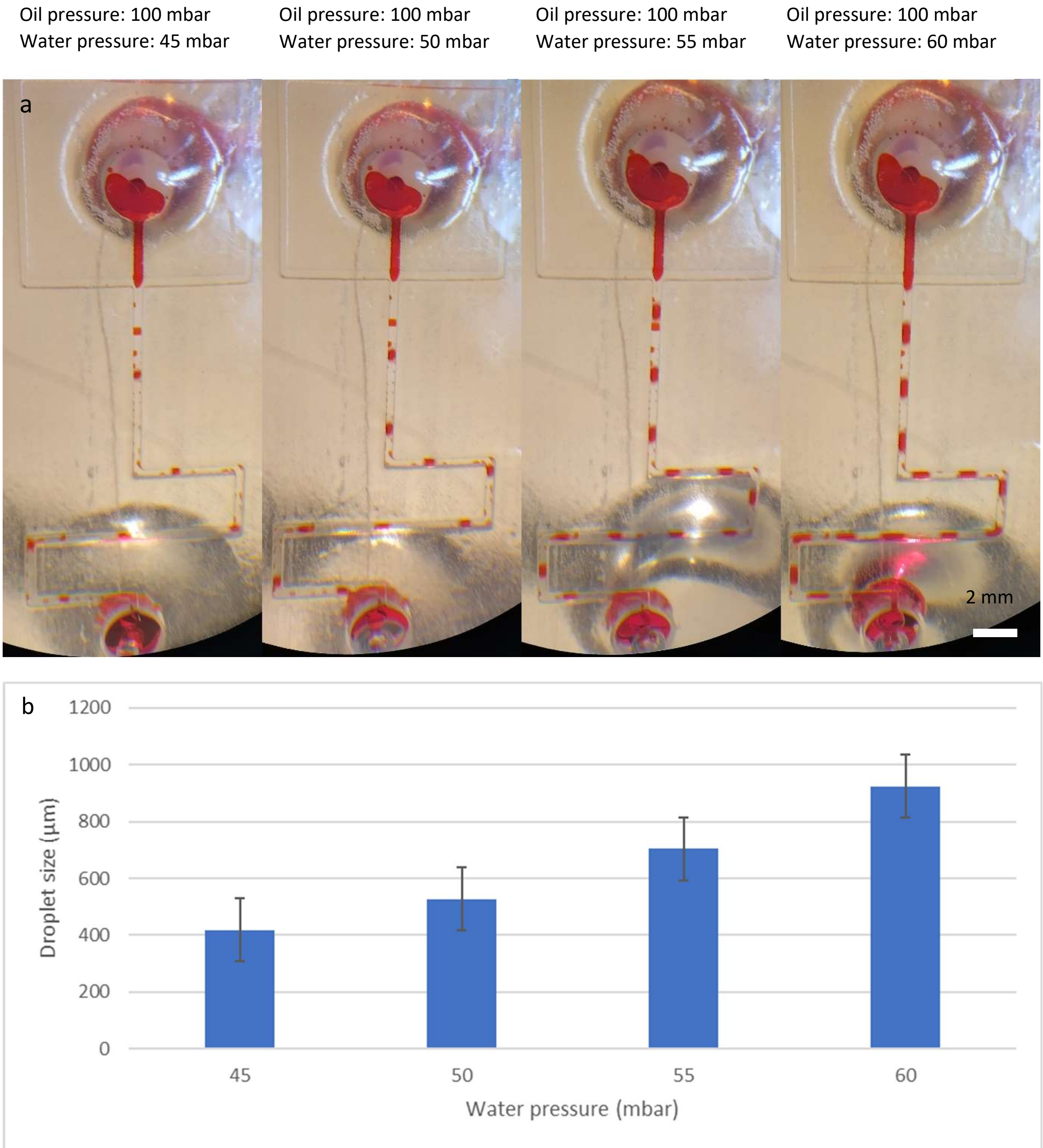

Figure 3 Water in oil droplets in a microchannel **(a)** Microscope photo microdroplets inside the channel for several water pressures. **(b)** Droplet size across water pressure.

A similar pattern showed itself at different oil pressure. At higher or lower oil pressure, by tuning the water pressure, droplet size increased or decreased which is similar to the experiment shown in Fig. 3. The only difference was the droplet formation frequency which is the out of scope of this work. Therefore, relative oil and water pressures affected the ratio of oil to water inside the microchannel.

Conclusion

Microdroplets were produced in a microchannel that has a flow-focusing geometry. Due to the hydrophilic composition of the 3D printed microchannels droplet production performance was lower than PDMS microchannels. The dripping regime was comparatively narrower than the hydrophobic channels too. The relative pressure of the water across oil pressure affected the droplet length inside the microchannel directly proportional. The total pressure of both fluids affected the droplet production frequency directly proportional as well.

Acknowledgments

This work was supported by the Scientific Research Projects Coordination Unit of Kırıkkale University. Project number 2021/043.

References

Bhargava, Krisna C, Bryant Thompson, and Noah Malmstadt (2014) Discrete elements for 3D microfluidics. Proceedings of the National Academy of Sciences 111(42):15013-15018.

Bilican, İsmail, and Mustafa Tahsin Guler (2020) Assessment of PMMA and polystyrene-based microfluidic chips fabricated using CO2 laser machining. Applied Surface Science 534:147642.

Donvito, Lidia, et al. (2015) Experimental validation of a simple, low-cost, T-junction droplet generator fabricated through 3D printing. Journal of Micromechanics and Microengineering 25(3):035013.

Ghorbanpoor, Hamed, et al. (2022) A fully integrated rapid on-chip antibiotic susceptibility test–A case study for Mycobacterium smegmatis. Sensors and Actuators A: Physical 339:113515.

Guler, M Tahsin (2022) Fabricating plasma bonded microfluidic chips by CO2 laser machining of PDMS by the application of viscoelastic particle focusing and droplet generation. Journal of Manufacturing Processes 73:260-268.

Guler, Mustafa Tahsin, Murat Inal, and Ismail Bilican (2021) CO2 laser machining for microfluidics mold fabrication from PMMA with applications on viscoelastic focusing, electrospun nanofiber production, and droplet generation. Journal of Industrial and Engineering Chemistry 98:340-349.

Isiksacan, Ziya, et al. (2016) Rapid fabrication of microfluidic PDMS devices from reusable PDMS molds using laser ablation. Journal of Micromechanics and Microengineering 26(3):035008.

Kecili, Seren, and H Cumhur Tekin (2020) Adhesive bonding strategies to fabricate the high-strength and transparent 3D printed microfluidic device. Biomicrofluidics 14(2):024113.

Kim, Tyson N, et al. (2005) Femtosecond laser-drilled capillary integrated into a microfluidic device. Applied Physics Letters 86(20):201106.

Kotz, Frederik, et al. (2018) Highly fluorinated methacrylates for optical 3D printing of microfluidic devices. Micromachines 9(3):115.

Lepowsky, Eric, Reza Amin, and Savas Tasoglu (2018) Assessing the reusability of 3D-printed photopolymer microfluidic chips for urine processing. Micromachines 9(10):520.

Li, Zhenqing, et al. (2023) Lower fluidic resistance of double-layer droplet continuous flow PCR microfluidic chip for rapid detection of bacteria. Analytica Chimica Acta 1251:340995.

Morgan, Alex JL, et al. (2016) Simple and versatile 3D printed microfluidics using fused filament fabrication. PloS one 11(4):e0152023.

Nelson, Matt D, Nirupama Ramkumar, and Bruce K Gale (2019) Flexible, transparent, sub-100 µm microfluidic channels with fused deposition modeling 3D-printed thermoplastic polyurethane. Journal of Micromechanics and Microengineering 29(9):095010.

Oliveira, Beatriz, et al. (2020) Fast prototyping microfluidics: integrating droplet digital lamp for absolute quantification of cancer biomarkers. Sensors 20(6):1624.

Tsuda, Soichiro, et al. (2015) Customizable 3D printed 'plug and play'millifluidic devices for programmable fluidics. PLoS One 10(11):e0141640.

Wu, Jiandong, et al. (2017) Lab-on-a-chip platforms for detection of cardiovascular disease and cancer biomarkers. Sensors 17(12):2934.